Quantum Information and Computation, Vol. 13, No. 3&4 (2013) 0324–0333
© Rinton Press

OPTICAL DETECTION OF QUANTUM ENTANGLEMENT BETWEEN TWO QUANTUM DOTS NEAR A METAL NANOPARTICLE

YONG HE* KA-DI ZHU†
Key Laboratory of Artificial Structures and Quantum Control, Department of Physics
Shanghai Jiao Tong University, Shanghai, China

Received May 7, 2012
Revised November 6, 2012

We theoretically study the interaction between two semiconductor quantum dots (SQDs) and a metal nanoparticle (MNP) within the quantum description. The plasmon field produced in the MNP excited by the external field can play the platform of Förster energy transfer between two SQDs which gives rise to the generation of entangled states. The Fano effect can be shown in the energy absorption spectrum of MNP, which originates from constructive or destructive interference between two competing optical pathways. Since the generated entangled state is in one pathway, the steady-state concurrence of entanglement can be evaluated by the observation of Fano profile. Because the concurrence of two SQDs is determined by both the pump intensity and the energy difference, one can properly choose these two parameters for detecting the non-negligible entanglement. When the pump intensity is very strong, there is no entanglement. The method to observe entanglement with the Fano profile, so, has a limited range of applicability. The optical observation is a novel approach to reveal entanglement. It may be used to optically detect quantum entanglement in many solid-state systems.

Keywords: Quantum entanglement, Fano effect
Communicated by: R Jozsa & J Eisert

1. Introduction

Entanglement is one of the most striking features of quantum physics, which has been studied extensively for showing its non-locality [1]. Entangled state is the essential resource in quantum information theory [2], and can be applied in quantum teleportation [3], quantum information processing [4], and so on. Various types of interactions can give rise to the generation of entanglement in many systems. Recently, the propagating plasmon field in one dimensional structure can be considered as a plasmonic waveguide which can interact with quantum emitters [5, 6], such as SQDs and atoms. Because of the plasmon-emitter interaction, quantum entanglement of two qubits near the plasmonic waveguide in a metal nanoring [7] or metal channel [8, 9] can be achieved. In principle, there are two descriptions for the exciton-plasmon interaction, i.e., semiclassical and quantum descriptions. Semiclassical description is that the exciton is described in the quantum framework while the description of the plasmon field is within the classical electromagnetic dynamics [10, 11]. However, the plasmon field has been quantized within quantum description for showing quantum effects

*heyong2010@sjtu.edu.cn
†Corresponding author: zhukadi@sjtu.edu.cn

[12, 13]. In a hybrid molecule consisting of a SQD and a MNP, Fano effect appears in the energy absorption spectrum as a result of the exciton-plasmon interaction. Comparison between the two descriptions for Fano effect of the coupled SQD–MNP system has been investigated [13].

In this article, we propose a hybrid molecule that consists of two SQDs and a MNP, and illustrate the exciton-plasmon interaction within quantum description [12] which originates from the energy transfer between SQD and MNP [14]. The interaction is related to the distance between them [15]. Because of the presence of the plasmon field, the optical properties of SQD can be modified. It shows the shifted energy and the decreased lifetime of the exciton in SQD [15, 16].

We show that the coupling of two SQDs can be realized mediated by the plasmon field in a MNP within quantum description of the exciton-plasmon interaction. In the excitation of an appropriate pump laser field, the entangled states can be populated in the hybrid molecule in the steady-state limit. Because an entangled state is in one of two competing optical pathways which create the Fano effect [17], the steady-state concurrence of entanglement can be evaluated by the observation of the Fano profile in the energy absorption spectrum. In order to detect the non-negligible entanglement, one can properly choose both the pump intensity and the energy difference.

2. Model and theory

The system under consideration is a hybrid molecule consisting of a spherical MNP with radius R and two identical spherical SQDs (SQD1 and SQD2) with the vacuum ground state $|0\rangle$ and the α-exciton state $|ex\rangle$ [10] in the presence of a pump laser field $E_0 = Ee^{-i\omega t} + c.c.$, as illustrated in Fig. 1.

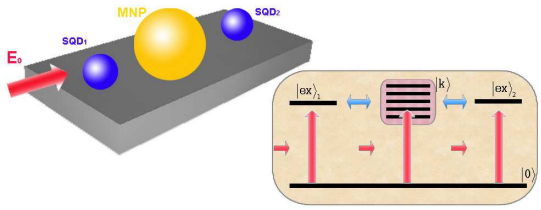

Fig. 1. Schematic illustration of a hybrid molecule consisting of two identical SQDs (SQD 1 and SQD 2) and a MNP in the presence of the pump laser field E_0. Inset shows quantum transitions (including photon-induced transition and coupling-induced transition) in the hybrid molecule.

The center-to-center distance between SQD1 (SQD2) and the MNP is d_1 (d_2). The entire system is embedded in a dielectric medium with dielectric constant ε_0. The Hamiltonian of the two SQDs can be written as:

$$H_{SQD} = \hbar\omega_{ex}\sigma^z, \tag{1}$$

where $\sigma^z = \sigma_1^z + \sigma_2^z$, $\sigma_i^z = (|ex\rangle_i\langle ex| - |0\rangle_i\langle 0|)/2$ $(i = 1, 2)$, ω_{ex} represents the transition frequency between the vacuum ground state and the exciton state. The plasmon field produced in the MNP can be quantized as a multi-modes field [12, 18]

$$H_p = \hbar\sum_k \omega_k a_k^+ a_k, \tag{2}$$

where ω_k is the frequency of mode k, a_k^+ (a_k) is the creation (annihilation) operation of mode k. Based on cavity quantum electrodynamics, each SQD can interact with the plasmon modes. Under the rotating-wave approximation the interaction Hamiltonian between SQD i and the plasmon modes can be written as [13, 18]

$$H_{int}^i = -\hbar \sum_k (g_k^i a_k \sigma_i^+ + h.c.), \tag{3}$$

where $\sigma_i^+ = |ex\rangle_i\langle 0|$, g_k^i is the coupling constant of SQD i and mode k. For simplicity, here, we assume $g_k^i = g_k$ which requires $d_i = d$. In the excitation of a pump laser field, the driving Hamiltonian is given by

$$H_D = -\{[(\mu/\varepsilon_{eff}) \sum_i \sigma_i^+ + \sum_k \mu_k^* a_k^+] E e^{-i\omega t} + h.c.\}, \tag{4}$$

where μ (μ_k) is the dipole moment between the ground state and the excited exciton state $|ex\rangle_i$ of SQD (the excited plasmon state $|k\rangle$ of MNP), $\varepsilon_{eff} = (\varepsilon_s + 2\varepsilon_0)/3\varepsilon_0$ is the screening factor with ε_s being the dielectric constant of SQD. So, the total Hamiltonian can be written as

$$\begin{aligned} H &= \hbar\omega_{ex}\sigma^z + \hbar \sum_k (\omega_k a_k^+ a_k) - \hbar \sum_k (g_k a_k \sigma^+ + g_k^* a_k^+ \sigma) \\ &\quad -\{[(\mu/\varepsilon_{eff})\sigma^+ + \sum_k (\mu_k^* a_k^+)] E e^{-i\omega t} + h.c.\}, \end{aligned} \tag{5}$$

where $\sigma^+ = \sum_i \sigma_i^+$. The full quantum dynamics of the hybrid molecule can be derived from the following master equation for the density operation

$$\hbar\partial_t \rho = -i[H, \rho] + \hbar(\varsigma_{SQD} + \varsigma_p), \tag{6}$$

where the Liouvillian terms $\varsigma_{SQD} = (\kappa/2) \times \sum_i (2\sigma_i \rho \sigma_i^+ - \sigma_i^+ \sigma_i \rho - \rho \sigma_i^+ \sigma_i)$ and $\varsigma_p = \sum_k (\gamma_k/2)(2a_k \rho a_k^+ - a_k^+ a_k \rho - \rho a_k^+ a_k)$ describe the various scattering channels of molecule decay, plasmon decay through Laudau damping, and radiative decay [18].

Based on Eq. (6), the expectation values A_k, B and $\langle a_k^+ a_k \rangle$ satisfy the following equations

$$\hbar\partial_t A_k = -i\hbar(\omega_k - \omega - i\gamma_k/2)A_k + i(\hbar g_k^* B + \mu_k^* E), \tag{7}$$

$$\hbar\partial_t \langle a_k^+ a_k \rangle = -\hbar\gamma_k \langle a_k^+ a_k \rangle - i[A_k(\hbar g_k B^* + \mu_k^* E) - c.c], \tag{8}$$

where $A_k = \langle a_k e^{i\omega t} \rangle$, $B = \langle \sigma e^{i\omega t} \rangle$. The above equations can not illustrate the dynamics of the entire system, but show the correspondence among some expectation values. In the steady state limit, making use of Eq. (7) we have $A_k = (\hbar g_k^* B + \mu_k^* E)/\hbar(\omega_k - \omega - i\gamma_k/2)$.

On the other hand, the semi-classical theory of the coupled SQD-MNP system, i.e., the exciton of SQD is described in the quantum framework while the plasmon field is in the classical electromagnetic dynamics, have been investigated for showing the optical properties [10, 11]. As described in Ref. [11], the Hamiltonian for the interaction between a SQD (SQD i) and the classical plasmon field is given by

$$H_i^c = \hbar\omega_{ex}\sigma_i^z - \mu E_{SQD}(\sigma_i + \sigma_i^+), \tag{9}$$

where $E_{SQD} = (\hbar/\mu)[(\Omega + G(\omega)B)e^{-i\omega t} + c.c.]$, $\Omega = [\mu/(\varepsilon_{eff}) + C(\omega)]E/\hbar$, $C(\omega) = \mu\gamma s_\alpha R^3/(\varepsilon_{eff}d^3)$, $G(\omega) = \gamma(\mu s_\alpha)^2 R^3/(\hbar\varepsilon_0\varepsilon_{eff}^2 d^6)$, $\gamma = (\varepsilon_m - \varepsilon_0)/(\varepsilon_m + 2\varepsilon_0)$, ε_m is the dielectric constant of MNP, $s_\alpha = 2(-1)$ for the exciton-dipole orientation parallel (perpendicular to) the axis of SQD i and MNP.

The semi-classical description of the exciton-plasmon interaction differs from its full quantum description because the plasmon field has been quantized in the latter. For finding the correspondence between the two descriptions, we take the trace over the quantized plasmon field, to obtain $Tr_p[H\rho] = \hbar\omega_{ex}\sigma^z - \{[\sum_k g_k A_k + (\mu E/\varepsilon_{eff})]\sigma^+ e^{-i\omega t} + h.c.\}$. Combining with Eq. (9), after the rotating-wave approximation we can obtain

$$\sum_k \mu_k^* \pi_k(\omega) = C(\omega), \sum_k g_k^* \pi_k(\omega) = G(\omega), \tag{10}$$

where $\pi_k(\omega) = g_k/(\omega_k - \omega - i\gamma_k/2)$. Since ω is arbitrary, we have $g_k = \theta\mu_k$, where $\theta = \mu s_\alpha/(\hbar\varepsilon_0\varepsilon_{eff}d^3)$ is a real number. The above equations show the correspondence between quantum and semi-classical descriptions for the exciton-plasmon interaction [13].

3. Decoupling using a quantum transformation

Now, we treat the density operation to obtain the reduced density operation of SQDs' subsystem. Firstly, we take a time-independent unity transformation e^s on the density operator ρ, where $s = \sum_k [\pi_k^*(\omega_{ex})a_k^+\sigma - \pi_k(\omega_{ex})a_k\sigma^+]$, so $\widetilde{\rho} = e^{-s}\rho e^s$. Combining with Eq. (6), we have $\hbar\partial_t\widetilde{\rho} = -i[e^{-s}He^s, \widetilde{\rho}] + \hbar e^{-s}(\varsigma_{SQD} + \varsigma_p)e^s$. We can see that in the mathematical expansions of the above equation the coupling between the plasmon modes and the SQDs mainly presents in the terms of order $O(g_k^3)$ and higher which can be neglected. For obtaining the reduced density operation of the SQDs $\rho_S = Tr_p[\widetilde{\rho}]$, we assume that the multiple-mode plasmon field can be considered as a thermal reservoir and the reservoir variables are distributed in the uncorrelated thermal equilibrium mixture of states [19], $\langle a_k^+ a_l\rangle = \overline{n}_k\delta_{k,l}$, where the thermal average boson number $(\overline{n}_k)^{-1} = exp[(\hbar\omega_k)/(k_BT)] - 1$, k_B is the Boltzmann constant, and T is the temperature. At low temperature, $\overline{n}_k \ll 1$. In the SQDs' subsystem, the master equation can be written as ($\hbar = 1$)

$$\partial_t\rho_S = -i[H_S, \rho_S] + \varsigma_S \tag{11}$$

where

$$H_S = \omega_0\sigma^z + G_0(\sigma_1^+\sigma_2 + \sigma_1\sigma_2^+) - (\mu_0 E\sigma^+ e^{-i\omega t} + c.c.), \tag{12}$$

$$\varsigma_S = \sum_{i,j=1,2} (\Gamma_{i,j}/2)(2\sigma_i\rho_S\sigma_j^+ - \sigma_i^+\sigma_j\rho_S - \rho_S\sigma_i^+\sigma_j), \tag{13}$$

$\omega_0 = \omega_{ex} - G_R$, $\mu_0 = \mu/\varepsilon_{eff} + C(\omega_{ex})$, $\Gamma_{1,1} = \Gamma_{2,2} = \kappa_0$, $\Gamma_{1,2} = \Gamma_{2,1} = \kappa_1$, $G_R = Re[G(\omega_{ex})]$, $G_I = Im[G(\omega_{ex})]$, $\kappa_0 = \kappa + 2G_I$, $\kappa_1 = 2G_I$. The above master equation illustrates the coupling of two SQDs (the coupling constant $G_0 = -G_R$). The quantized plasmon field produced in the MNP plays the platform of Förster energy transfer between two SQDs [20]. The master equation derived by the quantum transformation method is in good agreement with that of Ref. [8] which describes the interaction between two qubits mediated by one-dimensional plasmon field. In the SQDs' subsystem, we choose an adequate basic, i.e., $|1\rangle =$

$|0,0\rangle$, $|2\rangle = (|0,ex\rangle + |ex,0\rangle)/\sqrt{2}$, $|3\rangle = (|0,ex\rangle - |ex,0\rangle)/\sqrt{2}$, $|4\rangle = |ex,ex\rangle$. Based on Eq. (7), the exciton population M satisfies the following equations

$$\partial_t B = -i\{[\omega_0 - \omega - i(\kappa_0 + \kappa_1)/2] + G_R B(M-1) - 2\mu_0 E(M-1)\} \tag{14}$$

$$\partial_t M = -(\kappa_0 + \kappa_1)M - i(\mu_0 E B^* - c.c.) \tag{15}$$

Based on the above equations, we can obtain the steady-state solution $B = 2\Omega_0(M-1)/(K - i)$, where $K = 2[(\omega_{ex} - 2G_R - \omega) + MG_R]/(\kappa_0 + \kappa_1)$, $\Omega_0 = 2\mu_0 E/(\kappa_0 + \kappa_1)$. The exciton population M is determined by the following equation

$$(K^2 + 1)M + 2|\Omega_0|^2(M-1) = 0 \tag{16}$$

We exploit a quantum transformation to reduce the direct coupling between SQDs and MNP, so that their coupling are mainly included in the terms of high order which can be neglected for obtaining the master equation of SQDs' subsystem. This is a transformational decoupling treatment. After the treatment, however, the SQDs' subsystem is not considered as a closed system because the obtained steady-state solutions, such as M, have included "information" of the plasmon modes of MNP.

4. Fano effect

The energy transfer between SQDs and MNP occurs in the hybrid molecule [14, 21, 22]. The exciton energy can be transferred from SQDs to MNP, and then converted into heat [20, 23]. The energy absorption rate of MNP, $Q_M = \sum_k \hbar\omega_k\gamma_k\langle a_k^+ a_k\rangle/2$, can be obtained by Eq. (6). In the steady-state limit, Combining Eqs. (7) and (8) we have

$$\langle a_k^+ a_k\rangle = \frac{|g_k B|^2 + |\mu_k E|^2/\hbar^2 + 2Re[g_k^*\mu_k B]}{(\omega_k - \omega)^2 + \gamma_k^2/4}. \tag{17}$$

Since $g_k = \theta\mu_k$, ($\theta = \mu s_\alpha/(\hbar\varepsilon_0\varepsilon_{eff}d^3)$ is independent on the index k), we can obtain

$$Q_M = Q_0 \times \frac{(K - q_R)^2 + (q_I + 1)^2}{K^2 + 1}, \tag{18}$$

where $Q_0 = \sum_k \omega_k\gamma_k|\mu_k|^2E^2/\{2\hbar[(\omega_k - \omega)^2 + \gamma_k^2/4]\}$, $q_R = Re[q]$, $q_I = Im[q]$, $q = 4\theta(1 - M)\mu_0/(\kappa_0 + \kappa_1)$. Based on Eq. (10), $Q_0 = Im[\omega G(\omega)/\theta^2] = \omega\varepsilon_0 Im[\gamma]R^3E^2/2$ [13]. Eq. (18) shows a Fano function [24] with the generalized field–dependent complex Fano factor which includes both the nonlinear and dephasing effects [13]. However, the energy absorption rate of SQDs' subsystem is given by $Q_S = \hbar\omega_{ex}\kappa M/2$. As an example, we consider a Au MNP with radius $R = 7\ nm$, and its dielectric constant is $\varepsilon_M(\omega) = \varepsilon_b - \omega_p^2/[\omega(\omega + i\eta)]$ with $\varepsilon_b = 9.5$, $\hbar\omega_p = 9\ eV$, $\hbar\eta = 0.07\ eV$ [25]. The dielectric constant of the background medium is $\varepsilon_0 = 2$ (polymer), and $\varepsilon_s = 7.2$ (CdTe). And $s_\alpha = 2$. For the decay rate and the dipole moment of the exciton, we take $\kappa = 2.5\ GHz$, and $\mu = er_0$ with $r_0 = 0.65\ nm$. Here, the center-to-center distance $d = 35\ nm$ is chosen, so that the ratio $\Gamma_{1,2}/\Gamma_{1,1}$ equals about 0.3.

Fig. 2 shows the nonlinear Fano profile in the energy absorption spectrum of MNP in the strong pump laser field ($I_0 = 800\ W/cm^2$). The Fano interference refers to third sorts of states [17], i.e., the common ground state $|1\rangle$, an entangled state $|2\rangle$ and an infinite collection of

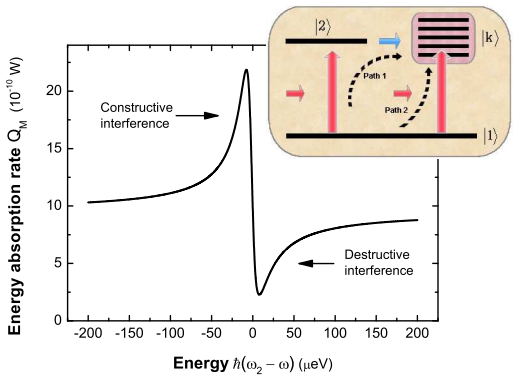

Fig. 2. The energy absorption rate of the MNP as a function of the energy difference $\hbar(\omega_2 - \omega)$ with the pump laser intensity $I_0 = 800\ W/cm^2$. Inset: Quantum interference pathways to excite the plasmon states $|k\rangle$ in the hybrid molecule in the steady-state limit.

extended states $|k\rangle$. As shown in inset of Fig. 2, there are two optical excitation transitions ($|1\rangle \rightarrow |2\rangle$ and $|1\rangle \rightarrow |k\rangle$) and one coupling transition ($|2\rangle \rightarrow |k\rangle$). Two optical pathways (path 1 and 2 in inset) can be found to generate the continuum of states $|k\rangle$. Constructive or destructive interference between two pathways, depending on the energy difference between quantum transition ($\hbar\omega_2 \equiv \hbar(\omega_{ex} - 2G_R)$ represents the quantum transition energy from $|1\rangle$ to $|2\rangle$) and the pump laser ($\hbar\omega$), give rise to the nonlinear Fano effect (see Fano function in Eq. (18)).

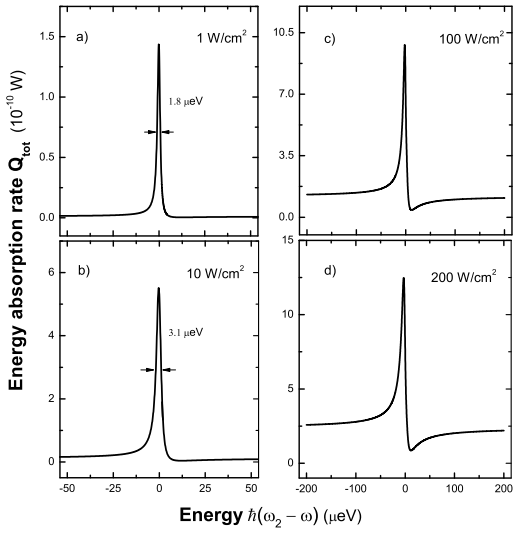

Fig. 3. The total energy absorption rate as a function of the energy difference $\hbar(\omega_2 - \omega)$ with different pump intensity I_0, (a) 1 W/cm^2, (b) 10 W/cm^2, (c) 100 W/cm^2, (d) 200 W/cm^2.

The total energy absorption rate of the entire system is given by $Q_{tot} = Q_M + Q_S$. In the weak field regime, the linear Fano effect appears in the total energy absorption spectrum.

Fig. 3a shows a symmetric peak with the broadening 1.8 μeV as the pump intensity I_0 = 1 W/cm^2. The exciton population $M \ll 1$ in the presence of weak pump laser field so that the Fano factor $q_R \gg 1$, which lead to the appearance of the symmetric peak profile [24]. However, the asymmetric Fano profile becomes more and more pronounced as the pump intensity increases. As shown in Figs. 3c and 3d, we can see the obvious nonlinear Fano effect as a result of the Fano interference. A strong pump laser field creates a large exciton population in SQDs' subsystem which give rise to the appearance of the nonlinear Fano effect. We find that the exciton population, which depends on the pump intensity, is a important factor in the determination of Fano profile. The entangled state $|2\rangle$ is a state in one of the two optical pathways that create Fano effect, which gives us a motivation to connect Fano profile with entanglement of two SQDs. Concurrence for quantifying entanglement of two SQDs, can be expressed as [8, 26]

$$C(t) = \sqrt{[\rho_{2,2}(t) - \rho_{3,3}(t)]^2 + 4Im[\rho_{2,3}(t)]^2}. \tag{19}$$

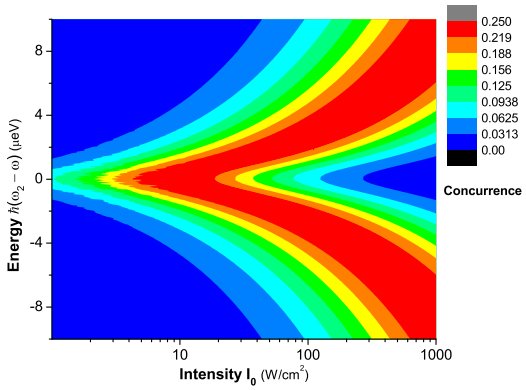

Fig. 4. The steady-state concurrence versus the energy difference $\hbar(\omega_2 - \omega)$ and the pump intensity I_0.

Fig. 4 plots the steady-state concurrence versus the energy difference $\hbar(\omega_2 - \omega)$ and the pump intensity I_0. The pump intensity and the energy difference can be obtained by analyzing Fano profile based on Fig. 3. Combining the two important parameters with Fig. 4, then, we can evaluate the steady-state concurrence. Because the entanglement of two SQDs is determined by both the pump intensity and the energy difference, according to the red region of Fig. 4, we can properly choose the two parameters to obtain the non-negligible entanglement. We can also see that the steady-state concurrence at resonance reaches the maximum value for every fixed intensity. At resonance $\omega_2 = \omega$, we plot the steady-state concurrence as a function of the pump intensity I_0. If the pump rate is much slower than the life of the state $|2\rangle$ (corresponding to a very weak pump intensity, such as 0.01 W/cm^2), the state $|2\rangle$ can be hardly populated so that the populations of the states $|2\rangle$, $|3\rangle$ and $|4\rangle$ can be neglected (the population of the state $|4\rangle$ is not more than that of the state $|2\rangle$ because of pumping from $|2\rangle$ to $|4\rangle$). This is the reason why the steady-state concurrence approximates to zero in the presence of very weak pump intensity. Because the transition frequency ω_2 from $|1\rangle$ to $|2\rangle$ is equal to the pump laser frequency ω (resonance, see the inset of Fig. 5),

the population of the state $|2\rangle$ can reach the saturation with an appropriate pump intensity (whose pump rate is much faster than the life of the state $|2\rangle$). Compared to the former, a stronger pump intensity is needed for the population of the state $|4\rangle$ to reach the saturation because of the non-resonance (see the inset of Fig. 5) between the pump frequency ω and the transition frequency ω_4 from $|2\rangle$ to $|4\rangle$ ($\omega_4 = \omega_{ex}$). And the population of the state $|4\rangle$ is connected to that of the state $|3\rangle$. With the increasing pump intensity, therefore, the steady-state concurrence firstly increases to reach the maximum value, then decreases. When the pump intensity is very large, such as 10000 W/cm^2, the populations of the three states, $|2\rangle$, $|3\rangle$ and $|4\rangle$ reach the saturation, and they are approximately equal so that the steady-state concurrence also approximates to zero. From Fig. 5, the steady-state concurrence reaches its maximum value at an optimal pump intensity, about 10 W/cm^2. However, the steady-state concurrence is small at strong pump intensity, such as 100 W/cm^2, 200 W/cm^2. So, at resonance we can choose an applicable pump intensity range (such as a range from 5 to 20 W/cm^2) for detecting the non-negligible entanglement.

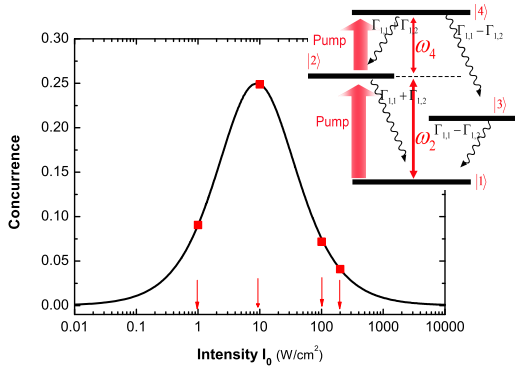

Fig. 5. The steady-state concurrence as a function of the pump intensity I_0 at resonance $\omega_2 = \omega$. Inset: The energy levels of two coupled SQDs.

Entanglement exists in various physical systems, such as entanglement based on photons [27], atoms [28], SQDs [7] and polymer molecules [29]. Quantum state tomography can be extensively used to measure the entangled state [2]. However, it is challenging in experiment because many copies of the measured states are necessary. The optical observation proposed by us, here, is a simple and feasible approach to obtain information of entanglement. And entanglement remains after the observation. The novel approach has potential to reveal entanglement in many solid-state systems. In Ref. [9], the authors demonstrated the generation of entanglement between two distant qubits mediated by the plasmonic waveguide, and proposed a scheme to detect the entanglement by measuring the cross terms of a second-order coherence function. Comparing with their scheme, our approach has the advantages in experiments because Fano effect in coupled exciton-plasmon system can be easily observed in experiments [30].

5. Conclusions

In conclusion, we have illustrated the coupling of two SQDs near a MNP which originates from

Förster energy transfer between the two SQDs mediated by the plasmon field in the MNP [20]. Because of the exciton-plasmon interaction the coupling among SQDs can give rise to the generation of entanglement [31], which is significant for quantum information science. In the excitation of a suitable pump laser field, one can achieve the steady-state entanglement. Concurrence of entanglement can be evaluated by optically observing Fano profile shown in the energy absorption spectrum. In order to detect the non-negligible entanglement of two SQDs, we can properly choose both the pump intensity and the energy difference. At resonance the maximum concurrence can be obtained at an optimal pump intensity. We also analyzed an applicable range of the pump intensity (such as an intermediate pumping range from 5 to 20 W/cm^2) which is important for detecting entanglement because there is no entanglement (concurrence is equal to zero) at a very strong pump intensity. Finally, we hope that our prediction in present work can be testified by experiments in the near future.

Acknowledgements

The authors gratefully acknowledge support from the National Natural Science Foundation of China under Grand No.10974133 and No.11274230 and the Ministry of Education Program for Ph.D..

References

1. R. Horodecki, P. Horodecki, M. Horodecki, and K. Horodecki (2009), *Quantum entanglement,* Rev. Mod. Phys., 81, pp. 865-942.
2. M. A. Nielsen and I. L. Chuang (2000), *Quantum computation and quantum information*, Cambridge University Press (Cambridge).
3. C. H. Bennett and S. J. Wiesner (1992), *Communication via one-and two-particle operators on Einstein-Podolsky-Rosen states,* Phys. Rev. Lett., 69, pp. 2881-2884.
4. S. B. Zheng and G. C. Guo (2000), *Efficient scheme for two-atom entanglement and quantum information processing in cavity QED,* Phys. Rev. Lett., 85, pp. 2392-2395.
5. M. L. Andersen, S. Stobbe, A. S. Sørensen, and P. Lodahl (2011), *Strongly modified plasmon-matter interaction with mesoscopic quantum emitters,* Nat. Phys., 7, pp. 215.
6. D. Dzsotjan, A. S. Sørensen, and M. Fleischhauer (2010), *Quantum emitters coupled to surface plasmons of a nanowire: A Greens function approach,* Phys. Rev. B, 82, pp. 075427.
7. Z. R. Lin, G. P. Guo, T. Tu, H. O. Li, C. L. Zou, J. X. Chen, Y. H. Lu, X. F. Ren, and G. C. Guo (2010), *Quantum bus of metal nanoring with surface plasmon polaritons,* Phys. Rev. B, 82, pp. 241401.
8. A. Gonzalez-Tudela, D. Martin-Cano, E. Moreno, L. Martin-Moreno, C. Tejedor, and F. Garcia-Vidal (2011), *Entanglement of two qubits mediated by one-dimensional plasmonic waveguides,* Phys. Rev. Lett., 106, pp. 020501.
9. D. Martín-Cano, A. Gonzalez-Tudela, L. Martin-Moreno, F. Garcia-Vidal, C. Tejedor, and E. Moreno (2011), *Dissipation-driven generation of two-qubit entanglement mediated by plasmonic waveguides,* Phys. Rev. B, 84, pp. 235306.
10. W. Zhang, A. O. Govorov, and G. W. Bryant (2006), *Semiconductor-metal nanoparticle molecules: Hybrid excitons and the nonlinear Fano effect,* Phys. Rev. Lett., 97, pp. 146804.
11. R. D. Artuso and G. W. Bryant (2010), *Strongly coupled quantum dot-metal nanoparticle systems: Exciton-induced transparency, discontinuous response, and suppression as driven quantum oscillator effects,* Phys. Rev. B, 82, PP. 195419.
12. U. Hohenester and A. Trügler (2008), *Interaction of single molecules with metallic nanoparticles,* IEEE J. Sel. Top. Quantum Electron., 14, pp. 1430.

13. W. Zhang and A. O. Govorov (2011), *Quantum theory of the nonlinear Fano effect in hybrid metal-semiconductor nanostructures: The case of strong nonlinearity,* Phys. Rev. B, 84, pp. 081405.
14. M. Kawai, A. Yamamoto, N. Matsuura, and Y. Kanemitsu (2008), *Energy transfer in mixed CdSe and Au nanoparticle monolayers studied by simultaneous photoluminescence and Raman spectral measurements,* Phys. Rev. B, 78, pp. 153308.
15. J. Lee, P. Hernandez, A. O. Govorov, and N. A. Kotov (2007), *ExcitonCplasmon interactions in molecular spring assemblies of nanowires and wavelength-based protein detection,* Nat. Mater., 6, pp. 291.
16. Y. Wang, T. Yang, M. T. Tuominen, and M. Achermann (2009), *Radiative rate enhancements in ensembles of hybrid metal-semiconductor nanostructures,* Phys. Rev. Lett., 102, pp. 163001.
17. M. Kroner, A. O. Govorov, S. Remi, B. Biedermann, S. Seidl, A. Badolato, P. M. Petroff, W. Zhang, R. Barbour, B. D. Gerardot, R. J. Warburton, and K. Karrai (2008), *The nonlinear Fano effect,* Nature, 451, pp. 311-314.
18. A. Trügler and U. Hohenester (2008), *Strong coupling between a metallic nanoparticle and a single molecule,* Phys. Rev. B, 77, pp. 115403.
19. M. O. Scully and M. S. Zubairy (1997), *Quantum Optics,* Cambridge University Press (Cambridge).
20. A. O. Govorov, J. Lee, and N. A. Kotov (2007), *Theory of plasmon-enhanced Förster energy transfer in optically excited semiconductor and metal nanoparticles,* Phys. Rev. B, 76, pp. 125308.
21. J. H. Song, T. Atay, S. Shi, H. Urabe, and A. V. Nurmikko (2005), *Large enhancement of fluorescence efficiency from CdSe/ZnS quantum dots induced by resonant coupling to spatially controlled surface plasmons,* Nano Lett., 5, pp. 1557.
22. T. Pons, I. L. Medintz, M. Sykora, and H. Mattoussi (2006), *Spectrally resolved energy transfer using quantum dot donors: Ensemble and single-molecule photoluminescence studies,* Phys. Rev. B, 73, pp. 245302.
23. A. Akimov, A. Mukherjee, C. Yu, D. Chang, A. Zibrov, P. Hemmer, H. Park, and M. Lukin (2007), *Generation of single optical plasmons in metallic nanowires coupled to quantum dots,* Nature, 450, pp. 402.
24. A. E. Miroshnichenko, S. Flach, and Y. S. Kivshar (2010), *Fano resonances in nanoscale structures,* Rev. Mod. Phys., 82, pp. 2257.
25. F. J. G. De Abajo (2009), *Optical excitations in electron microscopy,* Rev. Mod. Phys., 82, pp. 209.
26. W. K. Wootters (1998), *Entanglement of formation of an arbitrary state of two qubits,* Phys. Rev. Lett., 80, pp. 2245.
27. N. Kiesel, C. Schmid, G. Toth, E. Solano, and H. Weinfurter (2007), *Experimental observation of four-photon entangled Dicke state with high fidelity,* Phys. Rev. Lett., 98, pp. 63604.
28. J. Volz, M. Weber, D. Schlenk, W. Rosenfeld, J. Vrana, K. Saucke, C. Kurtsiefer, and H. Weinfurter (2006), *Observation of entanglement of a single photon with a trapped atom,* Phys. Rev. Lett., 96, pp. 30404.
29. J. Martin, M. Krutyeva, M. Monkenbusch, A. Arbe, J. Allgaier, A. Radulescu, P. Falus, J. Maiz, C. Mijangos, and J. Colmenero (2010), *Direct observation of confined single chain dynamics by neutron scattering,* Phys. Rev. Lett., 104, pp. 197801.
30. N. T. Fofang, N. K. Grady, Z. Fan, A. O. Govorov, and N. J. Halas (2011), *Plexciton dynamics: exciton-plasmon coupling in a J-aggregate-Au nanoshell complex provides a mechanism for nonlinearity,* Nano Lett., 11, pp. 1556.
31. Y. He, and K. D. Zhu (2012), *Strong coupling among semiconductor quantum dots induced by a metal nanoparticle,* Nanoscale Res. Lett., 7, pp. 95.